STEREOLOGICAL ANALYSIS OF MAMMALIAN SKELETAL MUSCLE

I. Soleus Muscle of the Adult Guinea Pig

BRENDA R. EISENBERG, AILEEN M. KUDA, and JAMES B. PETER

From the Department of Medicine, University of California at Los Angeles School of Medicine, Los Angeles, California 90024

ABSTRACT

A quantitative analysis of the volumes, surface areas, and dimensions of the ultrastructural components in the soleus muscle fibers of the guinea pig was made by using point counting methods of stereology. Muscle fibers have structural orientation (anisotropy) and have spatial gradients of the structures within the fiber; therefore the standard stereological methods were modified where necessary. The entire analysis was repeated at two section orientations to test the modifications and identical results obtained from both. The volume of lipid droplets was 0.20 ± 0.06% (mean ± standard error, n = 5 animals) and the nuclei volume was 0.86 ± 0.20% of the fiber volume. The total mitochondrial volume was 4.85 ± 0.66% of the fiber volume with about one-third being found in an annulus within 1 μm of the sarcolemma. The mitochondrial volume in the remaining core of the fiber was 3.6 ± 0.4%. The T system has a volume of 0.14 ± 0.01% and a surface area of 0.064 ± 0.005 $\mu m^2/\mu m^3$ of the fiber volume. The surface area of the sarcolemma is 0.116 ± 0.013 $\mu m^2/\mu m^3$ which is twice the T system surface area. The volume of the entire sarcoplasmic reticulum is 3.52 ± 0.33% and the surface area is 0.97 ± 0.09 $\mu m^2/\mu m^3$. The sarcoplasmic reticulum is composed of the terminal cisternae whose volume is 1.04 ± 0.19% and surface area is 0.24 ± 0.05 $\mu m^2/\mu m^3$. The tubules of the sarcoplasmic reticulum in the I band and A band have volumes of 1.97 ± 0.24% and 0.51 ± 0.08%, and the surface areas of the I and A band reticulum are 0.56 ± 0.07 $\mu m^2/\mu m^3$ and 0.16 ± 0.04 $\mu m^2/\mu m^3$, respectively. The Z line width, myofibril and fiber diameters were measured.

INTRODUCTION

All animals have muscles of various kinds which have evolved to suit particular functional roles. Anatomists and physiologists have examined many different muscles in order to understand and classify their various functions (Ranvier, 1874; Denny-Brown, 1929), and this work has been extended with the advent of the electron microscope. Our concern here is mammalian skeletal muscle which is under voluntary nervous control and exhibits twitch contractions. Much effort has been made to further classify the twitch fibers into different types. There are a number of papers on

fiber typing oriented to several disciplines: physiology (Peachey, 1968; Close, 1972; Burke et al., 1971), histochemistry (Edgerton and Simpson, 1969), biochemistry (Peter et al., 1972), and electron microscopy (Gauthier, 1970). The literature is contradictory and confusing because authors have used different criteria in their classification. Nonetheless fiber type classification is of clinical significance (Engel, 1970) because some diseases preferentially affect one type of motor unit, the fibers of which are of uniform type by histochemical criteria.

Quantitative anatomical studies should be helpful in correlating data from other disciplines. Many papers on the ultrastructure of skeletal muscle give only qualitative descriptions (Pellegrino and Franzini, 1963; Gauthier and Padykula, 1966; Shafiq et al., 1969; Ogata and Murata, 1969; Tomanek et al., 1973) while some are quantitative (Peachey, 1965; Schiaffino et al., 1970; Luff and Atwood, 1971; Galavazi and Szirmai, 1971; Mobley and Page, 1972; Hayashida and Schmalbruch, 1972; Kilarski, 1973; Herbener et al., 1973; and Stonnington and Engel, 1973).

Histochemical screening of fibers from many muscles of several species has shown that the soleus muscle of the adult guinea pig is composed entirely of slow-twitch-oxidative fibers (Edgerton and Simpson, 1969; Barnard et al., 1971). For this reason this muscle was chosen for a quantitative analysis by the point counting method of stereology (Weibel and Elias, 1967; Elias, 1967; DeHoff and Rhines, 1968; Underwood, 1970; Weibel, 1973). The relative simplicity of the soleus muscle permits empirical tests of the stereological technique and its application to oriented structures. A brief report of this research has appeared (Eisenberg et al., 1972).

THEORY OF STEREOLOGY APPLIED TO MUSCLE

A schematic drawing of a part of a mammalian muscle fiber (Fig. 1) shows the mitochondria, sarcolemma, components of the sarcoplasmic reticulum, and T system which are to be measured by stereological techniques. The nuclei, lipid droplets, and dimensions of the myofibrils and contractile proteins were also analyzed.

In classic stereological analysis one considers a three-dimensional volume of tissue containing randomly oriented organelles. The tissue is sectioned into flat slices for viewing in the electron microscope, and in a micrograph one observes numerous two-dimensional profiles of the organelles which will vary in shape, size, and orientation. The structure observed in the section is obviously related to that of the original tissue. For example, the probability of finding the profiles of mitochondria in the section will be that of finding the total volume of the mitochondria in the cell volume. Furthermore, the total boundary length of the mitochondrial profiles in the flat section will bear a simple relationship to their surface area in the cell volume. Geometric probability theory can be used to calculate the average three-dimensional volumes and surface areas from the observed two-dimensional images for these isotropic structures.

However, when the organelles are oriented with respect to one another, a single micrograph will contain anisotropic profiles of the organelles which are identical in shape, size, and orientation. For example, when a volume contains cylinders, cross-sections yield sets of circles, oblique sections yield ellipses, and longitudinal sections yield parallel lines. Nonetheless the profiles still occur with the same frequency as the occurrence of the cylinders in the cell volume, and the volume of the cylinders will be correctly estimated by the formula derived for the isotropic case. However, the relationship between the boundary length of the two-dimensional circles and the three-dimensional cylinders will be different from the isotropic case and indeed will be different for the ellipses or parallel lines. The exact relationship will depend on the statistical distribution of the orientation of the cylinders and also on the sectioning plane.

A muscle fiber is anisotropic because the fibrils are fully oriented. Therefore we did not feel justified in applying the simple isotropic theory. However, one cannot assume the degree and distribution of the orientation of a particular organelle without empirical testing and theoretical analysis. We therefore performed the entire stereological analysis in two orientations using both longitudinal and cross sections. In addition, consideration has been taken of systematic errors caused by the finite thickness of the section. Furthermore, the distribution of the organelles within the cell and within the striation patterns has been discussed.

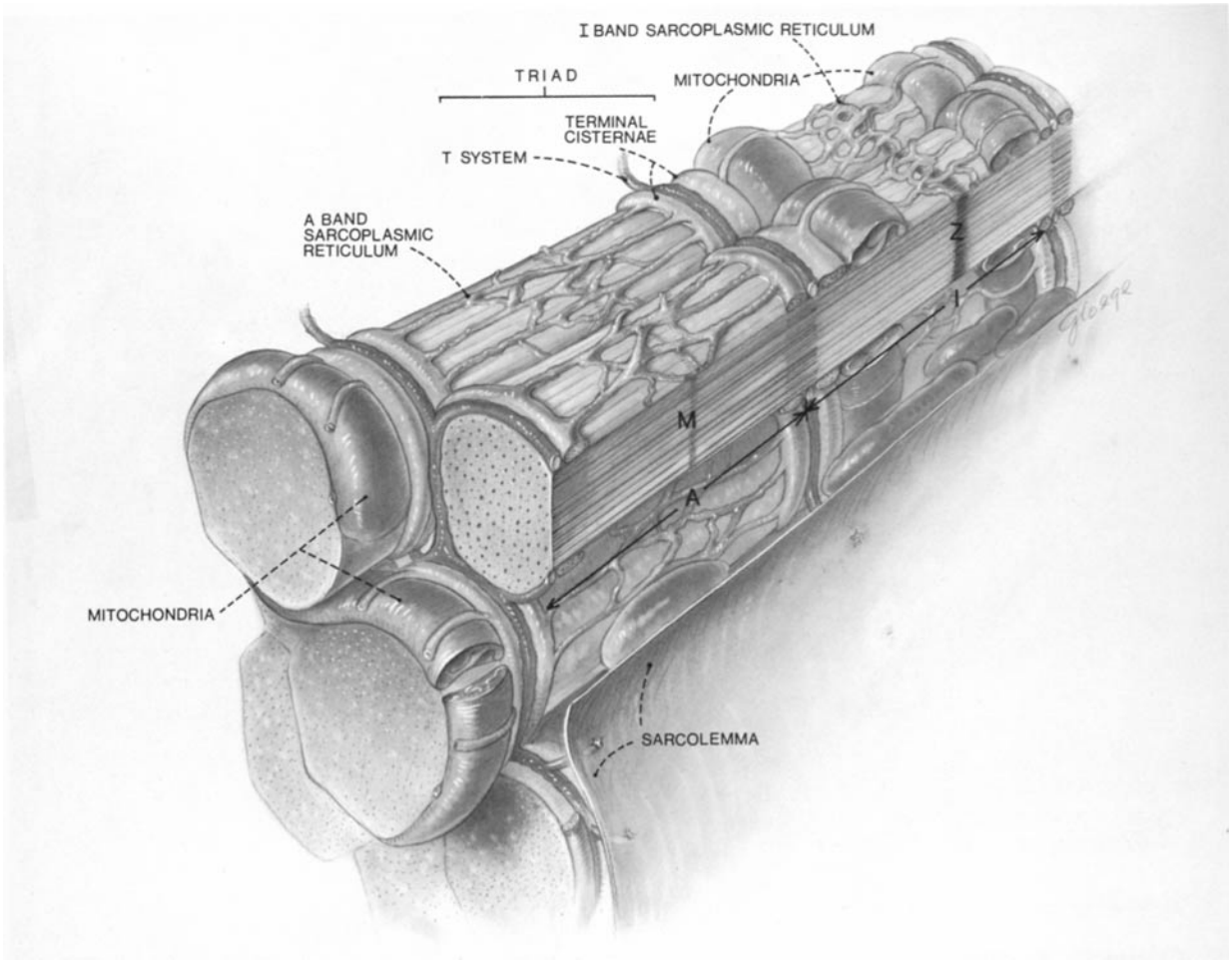

FIGURE 1. A schematic drawing of part of a mammalian skeletal muscle fiber.

Volume Density in Isotropic Tissue

Several reviews and books have been devoted to the theory of stereology and its application to biological sections (Weibel, 1963; Weibel and Elias, 1967; Elias, 1967; DeHoff and Rhines, 1968; Weibel, 1969; Underwood, 1970; Elias et al., 1971), and derivations can be found in them to show that the volume fraction or volume density V_v is given by:

$$V_v = \frac{V_1}{V_2} = \frac{\bar{A}_1}{\bar{A}_2} = \frac{\bar{L}_1}{\bar{L}_2} = \frac{\bar{P}_1}{\bar{P}_2}, \qquad (1)$$

where $\bar{A}$ refers to the mean area,[1] $\bar{L}$ to the mean line length, and $\bar{P}$ to the mean point counts of the components 1 and 2, respectively. Note that in Eq. 1 the estimate of volume fraction (V_v) is independent of the shape of the structure being studied, if the material being tested is randomly selected, the sections are infinitely thin, and the tissue is homogeneous.

Volume fractions (V_v) measured by point counting methods generally are expressed as $V_{v1} = V_1/V_2$ which is defined as the volume of test objects V_1 per unit reference volume of tissue V_2 (International Stereology Society usage: Weibel and Elias, 1967). However, we sometimes refer object volumes V_1 to a different reference volume V_3. This is undefined in the International terminology, but might be rendered as $V_{v_{2_1}}$ and $V_{v_{3_1}}$ which are difficult to read and whose meaning is unclear. We therefore retain the simple fractional notation of V_1/V_2 or V_1/V_3 throughout this paper

[1] Note that $\bar{A}$ refers to the mean profile area and should not be confused with A which refers to the A band of the muscle fiber.

for clarity. The surface densities are similarly given by the symbol S_1/V_2 or S_1/V_3 by us, instead of the International system of $S_{v_{2_1}}$ and $S_{v_{3_1}}$.

Volume Density in Anisotropic Tissue

Weibel (1972) has shown that in oriented tissue there should be no dependence of the volume density on the angle ϕ which is the angle the section subtends with the axis of the fiber because:

$$\frac{V_1}{V_2} = \frac{K(\phi)\cdot\bar{A}_1}{K(\phi)\cdot\bar{A}_2} = \frac{\bar{A}_1}{\bar{A}_2}, \tag{2}$$

where K (ϕ) is some function of the sectioning angle ϕ. Hence on both theoretical and experimental grounds Eq. 1 can be used to estimate volume density from point counting of anisotropic tissue.

In striated material it is important to ensure that the point counts from the test grid are independent of the geometrical arrangement and spacing of the grid. The quadratic test grid chosen for our analysis has parallel sets of points spaced d micra apart (Fig. 5). Longitudinally sectioned muscle tissue also has parallel striations spaced at sarcomere intervals, s, about 3.4 μm apart. The angle between the test grid lines and the sarcomeres is $\theta°$ and $(90 + \theta)°$, which are called the test grid angles and are distinct from ϕ the sectioning angle. There is a possibility of maximal interference between the test grid and sarcomere repeat when $\theta = 0°$ and 90° and d = 3.4 μm that all the points will sample from only one of the bands. In general the interference will depend on "$d \sin \theta$" in a manner similar to optical interference (Bragg's Law). Empirical tests were made of orientation and interference effects with the chosen test grid rotated to various angles θ. We observed no dependence of the point counts and so of the volume estimates on θ, perhaps because in our case the test lines were sufficiently close that several samples were taken within one band of each sarcomere.

Surface Density in Isotropic Tissue

The boundary length of surface $(\bar{B})$ per unit area $(\bar{A})$ of the micrograph is related to the surface area per unit volume of the tissue by the geometry or shape of the surface. For isotropic surfaces Smith and Guttman (1953) derive

$$\frac{\bar{B}}{\bar{A}} = \frac{\pi}{2}\cdot\frac{\bar{C}}{L}, \tag{3}$$

where $\bar{C}$ is the mean number of intersections[2] made between the surface of the object and the total test line length (L).

The surface density (S_v) is the surface area per unit volume, and for randomly oriented objects has been shown to be

$$S_v = \frac{S}{\bar{V}} = \frac{2\bar{C}}{L}. \tag{4}$$

Eq. 4 has been derived many times (Underwood, 1970, p. 31). Combination of Eqs. 3 and 4 gives:

$$\frac{S}{\bar{V}} = \frac{4\bar{B}}{\pi\bar{A}}. \tag{5}$$

The total test line length (L) in our system is

$$L = 2q^2\, d\, P, \tag{6}$$

where q is the ratio of heavy to light points, d is the spacing between the light test lines in micra, and P is the number of heavy points falling on the muscle (Weibel, 1972). Hence,

$$\frac{S}{\bar{V}} = \frac{\bar{C}}{q^2 dP}. \tag{7}$$

Eq. 7 can be used to give an estimate of the surface density of a component when random sampling of sufficient area of tissue is made and when the surfaces are isotropic.

Surface Density in Anisotropic Tissue

The boundary length and the area within the boundary of oriented structures will appear to change when the sectioning angle ϕ is changed, and the change will depend on the geometry of the model chosen to represent the structure. For example, consider section planes through parallel rods of square cross sections at various angles ϕ, the resulting ratio of boundary length to enclosed area $(\bar{B}/\bar{A})$ is $2(1 + \sin \phi)/a$, where a is the length of the side. For parallel circular cylinders of

[2] The International Stereological Society uses I for intersection counts but in muscle studies I means I band, therefore C is used for intersection counts.

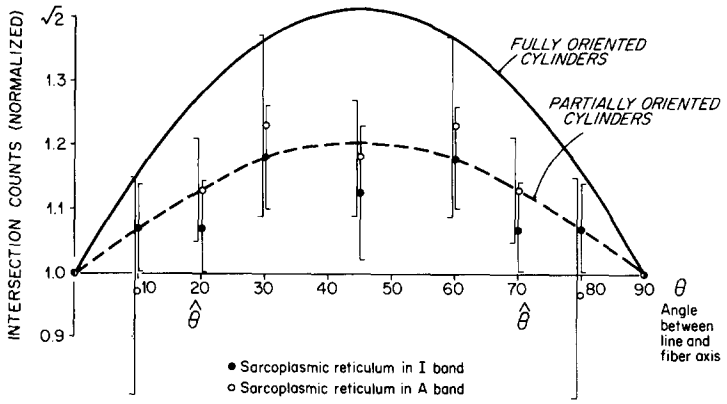

FIGURE 2 The solid line shows the relationship between the intersection counts and $f(\theta) = \sin\theta + \cos\theta$ for fully oriented surfaces, where θ is the angle between one set of parallel test grid lines and the fiber axis. The orthogonal set of test lines make the angle $(\theta + 90°)$ with the fiber axis. For randomly oriented cylinders the intersection counts would be independent of θ and equal to a value of 1.0 for all θ. The dotted curve is drawn through experimentally determined data for the I and A band sarcoplasmic reticulum and shows only a partial orientation of the sarcoplasmic reticulum surface with respect to the fiber axis.

diameter c,

$$\frac{\bar{B}}{\bar{A}} = \frac{4}{c}\sqrt{\frac{1+\sin^2\phi}{2}}, \qquad (8)$$

an equation derived by Weibel in another form (Eq. 36, Weibel, 1972). Experimentally one must guess a model shape in order to determine which equation for $\bar{B}/\bar{A}$ will best apply. Only then can an estimate of $\bar{B}/\bar{A}$ be made. Furthermore, the number of intersection counts (C) made between parallel test lines and the oriented surface will change with the sectioning angle ϕ and with the test grid angles θ.

If orientation exists, several experimental approaches are available. The sections may be taken at random sectioning angles ϕ and averaged over many angles. The mean number of intersection counts $\bar{C}$ at random θ can be determined by rotating the test grid to several positions on each micrograph (Sitte, 1967; Mobley and Page, 1972). Curvilinear grids ensure that all test surfaces will be crossed at all θ in a random manner and hence $\bar{C}$ will be determined from any position of counting. Zig-zag test grids (Santa et al., 1972) have straight line portions and are subject to orientation errors. A theoretical discussion is given by Hilliard (1967).

The approach we have taken is due to Sitte (1967) and makes use of a known, fixed sectioning angle ϕ and the fact that the quadratic line test grid can be placed at an "optimal angle" $(\bar{\theta})$ to yield the mean number of counts $(\bar{C})$. The dependence of C on θ for one set of the quadratic test grid lines is proportional to $\sin\theta$ and for the orthogonal lines is proportional to $\sin(90° + \theta) = \cos\theta$. Therefore the number of counts from both lines is given by

$$f(\theta) = R(\sin\theta + \cos\theta), \qquad (9)$$

where R is a proportionality constant. This function of the number of counts vs. θ has often been plotted on polar coordinate paper (the "rose" plot-Underwood, 1968) although we prefer a more simple linear graph (Fig. 2).

This plot shows that the counts observed at $\theta = 0°$ and $90°$ will be less than the mean, whereas at $\theta = 45°$ they will be more than the mean. Between these extremes lies a value $\bar{\theta}$, the "mean" value of the angle θ, at which angle the correct mean value of $\bar{C}$ will be measured.

The mean value theorem (Courant, 1937, p. 127) gives:

$$\frac{\pi}{2} Rf(\bar{\theta}) = \int_0^{\pi/2} R(\sin\theta + \cos\theta)\, d\theta = 2R,$$

where $f(\bar{\theta})$ is a function of θ and

$$f(\bar{\theta}) = \frac{4}{\pi}.$$

The mean value of $\bar{\theta}$ is then given by

$$\cos \bar{\theta} + \sin \bar{\theta} = \frac{4}{\pi}, \tag{10}$$

which is satisfied by $\bar{\theta} = 19°$ and 71°, the optimal angles of Sitte. Therefore placing the quadratic grid with one set of lines at $\bar{\theta} = 19°$ and the other at $\bar{\theta} = 71°$ to the orientation axis should give the correct mean value of the number of intersections for fully oriented surfaces. Fig. 2 also shows results for the intersection counts for the elements of the sarcoplasmic reticulum at the various angles θ. The curves clearly indicate that anisotropy is present. Therefore measurements were made with the grid oriented at the angle $\bar{\theta}$. In practice this was done by drawing a line at 19° and 71° directly on the quadratic test sheet. This line is then aligned with the orientation axis of the filaments of each micrograph.

Having determined the mean value of the intersection counts ($\overline{C}$), we may return to the problem of relating $\overline{C}$ to the boundary length $\overline{B}$ in area $\bar{A}$ and hence to the surface density S/V of the test object per unit volume. Weibel (1972) has analyzed the model of parallel circular cylinders and has shown that:

$$\frac{S}{V} = \frac{1}{k(\phi)} \cdot \frac{\bar{B}}{\bar{A}} = \frac{1}{k(\phi)} \cdot \frac{\pi \bar{C}}{2L}, \tag{11}$$

where

$$k(\phi) = \frac{\sqrt{\frac{1 + \operatorname{cosec}^2 \phi}{2}}}{\operatorname{cosec} \phi} = \sqrt{\frac{1 + \sin^2 \phi}{2}}, \tag{12}$$

which is the ϕ-dependent part from Eq. 8. Note that at $\phi = 90°$, $k(\phi) = 1$, and for cylinders cut in cross section:

$$\frac{S}{V} = \frac{\pi \bar{C}}{2L} = \frac{\pi \bar{C}}{4q^2\, dP}. \tag{13}$$

Longitudinal sections at $\phi = 0°$ give $k(\phi) = 1/\sqrt{2}$ and hence:

$$\frac{S}{V} = \frac{\sqrt{2}\pi \bar{C}}{4q^2\, dP}. \tag{14}$$

The above discussion of anisotropy will enable us to relax the theoretical restriction of random orientation which is assumed in the standard stereological derivations. We must now consider the second restriction, namely that the section be infinitely thin.

Section Thickness Effect

In practice our electron microscope sections are between 0.06 and 0.09 μm thick as judged by interference colors (Peachey, 1958). This thickness is comparable, for instance, to the diameter of the tubules of the sarcoplasmic reticulum, and so one expected errors to be introduced. Micrographs are flat images onto which three-dimensional structures have been projected. Consequently, uncritical use of Eq. 1 for such thin structures will result in errors; for example, the volume fraction of opaque structures will be overestimated and the translucent structures observed will be underestimated. However, correction factors can be determined (Holmes, 1927; Underwood, 1970, p. 174) which when multiplied by the apparent estimate will give a correct result. These correction factors depend on the shape, orientation, surface-to-volume ratio of the structure being measured, and the statistical distribution of these components, as well as on the ratio of the diameter (a) of the structure to the section thickness (t). Since these various parameters are often unknown, and since the statistical distribution of the parameters are almost never known, it seems somewhat unprofitable to try to determine in detail a correction factor appropriate for our situation. Rather, we set bounds on the errors produced by the naive application of Eq. 1.

Our worst problem occurs in the estimation of the parameters of the sarcoplasmic reticulum because the tubules of the reticulum are of about the same diameter (a) as the section thickness (t). If these cylinders are cut transversely, there is, of course, no error, so such measurements need not be corrected. If the cylinders are cut longitudinally, the correction factor will be less than $\pi a/4t$ or about 0.7 for the tubules of sarcoplasmic reticulum. This number is calculated assuming the cylinders are oriented strictly parallel to the section and lie entirely within the section.

However, the correction factor just determined must be modified because of other effects. Profiles formed by grazing the surface of the test object will be very small in size and therefore will not

be identified. We can estimate the size of this identification effect from Loud's data for the loss of membrane image in oblique sections (Loud, 1967). The identification problem produced errors in the opposite direction from the section thickness effect, but we find on theoretical grounds that the two errors are about the same size. We therefore assume they cancel and use the unmodified Eq. 1 directly. Data from transverse sections is less subject to these errors than that from longitudinal sections.

Spatial Gradients

Within a single fiber there are two examples of spatial gradients of structures (DeHoff in Elias, 1967, p. 119) which cause problems when fiber type histograms are to be constructed. The fibers are striated and have higher densities of lipid droplets and mitochondria near the cell periphery. We chose to exclude the peripheral 1-μm annulus and construct our histograms from the remaining core of the fibers. This avoided the sampling problems caused by structural gradients in the peripheral region. Representative sampling from both bands of the sarcomere in one micrograph is essential if cell structures within one band are to be referred to the total fiber volume (Weibel, 1972). This does not generally occur, for example, in longitudinally sectioned muscle at 30,000 ×, where only two or three sarcomeres are sampled and the error in the volume estimate of one band could be 25%. In these cases the volume of the structure, for example the sarcoplasmic reticulum in the I band, V_{srI}, can be referred to the volume of the I band (V_I) without error. Thus, we measure V_{srI}/V_I and determine the volume fraction referred to the volume of the fiber (V_F):

$$\frac{V_{srI}}{V_F} = \frac{V_{srI}}{V_I} \times \frac{V_I}{V_F}, \qquad (15)$$

where V_I/V_F is estimated by measuring the ratio of the lengths of the I band to the sarcomere length; see Eq. 1.

In oblique sections, especially cross sections the errors of structural gradients within the sarcomere are even more serious. The apparent sarcomere length in such sections is given by $s \cos \phi$ where the true sarcomere length is s and ϕ is the angle between the plane of section and the fiber axis. Cross sections in which the sectioning angle approaches 90° include very few sarcomeres. We follow the procedure of estimating V_{srI}/V_I from each fiber, and determining V_{srI}/V_F from Eq. 15 using the *mean* value of V_I/V_F determined by point counting from many fibers. This procedure cannot be used to form a meaningful fiber-by-fiber histogram of the volume fraction of the sarcoplasmic reticulum in the A and I bands.

MATERIALS AND METHODS

Fixation

Five male, mixed-breed guinea pigs weighing between 400 and 600 g were anesthetized by intraperitoneal injection of 50 mg/kg of Nembutal. The soleus muscle was carefully dissected and split into two or three longitudinal pieces, such that the diameter of each piece was not more than 2 mm. The pieces were tied at rest length to toothpicks and submerged in the fixative (5% glutaraldehyde in 0.1 M sodium cacodylate buffer pH 7.2 plus 2 mM $CaCl_2$). The time from interruption of the blood supply to submersion in the fixative was not more than 5 min. After 1½–2 h in the glutaraldehyde fixative at room temperature the entire muscle was trimmed, rinsed in a buffer wash for 10–15 min (0.1 M sodium cacodylate plus 2 mM $CaCl_2$ plus 10% sucrose) before postfixation in a 1% osmium tetroxide solution with 0.1 M sodium cacodylate buffer, pH 7.2. A 2-h soak in 1% aqueous uranyl acetate solution for en bloc staining preceeded dehydration through a graded series of ethanols and infiltration with Epon. In one experiment the muscle was cut in half and the second half was frozen for histochemistry, kindly performed for us by Dr. V. R. Edgerton. Frozen sections were used for size comparisons with fibers embedded in Epon.

Sampling

10 blocks of tissue were randomly selected by the method of Weibel et al. (1966) from each soleus muscle. Five were embedded in flat molds for subsequent transverse sections and five were embedded in inverted gelatin capsules for longitudinal sections.

Sectioning

Blocks were trimmed for thin sectioning in a nonselective manner, except that areas were rejected when judged grossly swollen or damaged in the light microscope. Uniform thin sections of a silver-gray interference color (600–900 Å thick) were taken with the LKB-Huxley microtome. The sections were heavily stained with saturated uranyl acetate and lead citrate (Venable and Coggeshall, 1965). The size of the thin section was measured under phase optics and compared with the size of the block face.

Compression along the direction of the knife edge was negligibly small. Compression perpendicular to the knife edge was 5.6 ± 0.2%, n = 10. The fiber axis of the muscle in the longitudinal sections parallels the knife edge, thus the width of the Z band and filament lengths will not be compressed (Page and Huxley, 1963).

Electron Microscopy

A Siemens Elmiskop 1A was modified so that the currents in the objective, intermediate, and projector lenses (Dunn and Preiss, 1973) could be measured with a digital ammeter. Care was taken to normalize all lens currents by turning the lens off and on three times to avoid magnetic hysterisis. Calibration checks with a carbon replica grating showed that the absolute magnification was reproducible to better than 1% over a period of 1 yr. Distortion caused by lens aberrations was found to be less than 2%.

Measurements from Cross Sections of Muscle Fibers

LIGHT MICROSCOPY: 1-μm thick sections from untrimmed blocks were taken with the LKB-Huxley microtome, stained with toluidine blue, and observed with the Zeiss RA light microscope. The orientation angle ϕ was estimated by noting the apparent sarcomere repeat $s \cos \phi$ (Page and Huxley, 1963). Within a typical block face of tissue cut in cross section the angle can vary from ϕ = 90°–50°, since the fibers tend to spiral or bend from one region to another (Fig. 3). Fibers were rejected if the angle was less than 75°. Sections were defocused at low magnification and the slide was randomly moved until the tissue was in view. The area was then refocused under oil immersion (× 1000) and point counting was done using a 10 × 10 net reticule in the eyepiece. Points falling on the capillaries, muscle cell nuclei, and muscle cytoplasm were determined at this magnification and used in volume calculations. Fiber diameter was determined from photographs printed at a final magnification of 750.

LOW MAGNIFICATION ELECTRON MICROSCOPY (× 12,000): Micrographs were taken according to the raster pattern scanning rules of Weibel et al. (1966) so that corners of the 300-mesh copper grid having muscle cell components in them were photographed and printed to give a final magnification of 12,000. Three micrographs from each of the 25 blocks were made.

A double-test grid with light lines every 0.4 μm and every fifth line heavy was randomly oriented to the micrograph. The grid ratio q of light-to-heavy lines is 5. The heavy points were used to make counts for A band (P_A) and I band (P_I) contained in the core of the fiber (Fig. 5). All the points, both heavy and light, were used to estimate the smaller areas of the outer 1-μm annulus (P_O). All points were also used to determine the rarer cytoplasmic components such as the lipid droplets (P_{lip}), the nuclei (P_{nuc}), the mitochondria in the periphery (P_{mitO}), the mitochondria in the A band (P_{mitA}), and in the I band (P_{mitI}). Points falling on mitochondria at the boundary between A and I bands were tallied separately and half assigned to each band. Grazing sections of mitochondria can be confused with terminal cisternae; similarly only half of these counts were assigned to the mitochondrial fraction.

The sarcolemmal surface area was estimated by recording the intersection counts C_F with all the light and heavy test lines.

HIGH MAGNIFICATION ELECTRON MICROS-

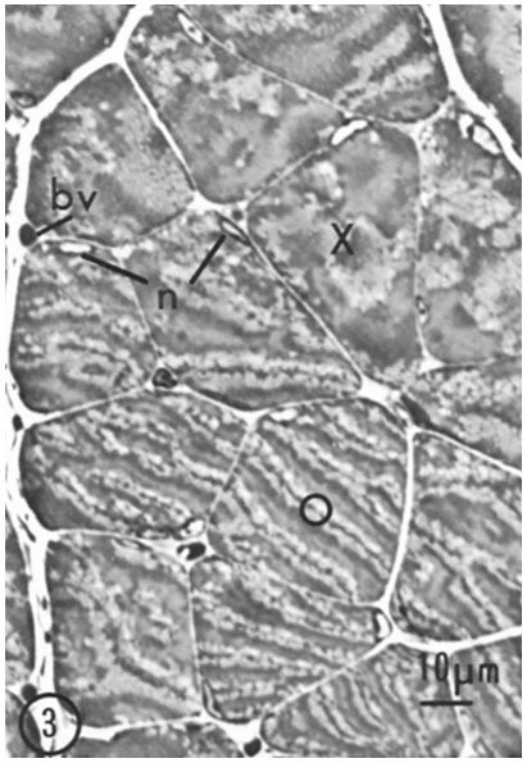

FIGURE 3 Light micrograph of soleus muscle in cross section. The fibers are irregularly shaped and contain peripheral nuclei (n). Note the small blood vessels (bv). The dark A band, light I band, and Z disk vary in orientation from one fiber to another, giving the fibers a marbled appearance. The pattern in fiber X is formed from only one A and one I band, indicating a nearly true cross section (ϕ = 90°), whereas in fiber O the striation patterns indicate an oblique section at the angle of (ϕ = 75°). × 750.

COPY (× 30,000): High magnification (30,000) was used to estimate small components within one fiber. The angle ϕ at which the block was oriented gave an apparent sarcomere repeat of 7 μm or less, the whole of which could be covered by two adjacent micrographs at × 30,000. The first micrograph was taken in the corner of the grid and the second was adjacent in the direction of the sarcomere repeat. Three fibers were used from each block. The double test grid with light lines every 0.17 μm was randomly placed on the micrograph. The heavy points were used to count the I band (P_I) and A band (P_A). The light and heavy points were used to determine the sarcoplasmic reticulum in the I band (P_{srI}) and in the A band (P_{srA}), the terminal cisternae (P_{tc}), and the transverse tubules (P_{tt}). The intersection counts of the light and heavy lines with the surfaces of I band and A band sarcoplasmic reticulum (C_{srI} and C_{srA}), terminal cisternae (C_{tc}), and transverse tubules (C_{tt}) were made. Tangential lines to a surface were recorded as one, not two counts. The entire counting procedure from one micrograph at ×30,000 took approximately 5 min.

Terminal cisternae are recognizable by their granular content. The tubules sandwiched between the cisternae, running transversely to the muscle fiber axis, are defined as transverse tubules. Tubules elsewhere were assigned to the sarcoplasmic reticulum and classified according to the band in which they lie. Errors in recognition of meandering T tubules cannot be determined without the aid of an extracellular marker such as peroxidase.

The myofibril diameters from cross-sectioned muscle were determined by measuring the major and minor axes from 53 myofibrils in five micrographs and calculating a mean diameter.

Measurements from Longitudinal Sections of Muscle Fibers

LIGHT MICROSCOPY: Sections of guinea pig soleus muscle were considered to be longitudinally oriented when the fibers had parallel sides for the entire width of the block face. For simple right circular cylinders of equal size the mean profile diameter $\bar{L}$ is related to the mean fiber diameter $\bar{D}$ by the equation from Elias and Hennig (1967).

$$\bar{L} = \frac{\pi}{4}\bar{D} \tag{16}$$

The profile diameters of 246 fibers were measured at × 1000 with oil immersion optics using a micrometer in the eyepiece thus permitting the diameter to be estimated from longitudinal sections.

LOW MAGNIFICATION ELECTRON MICROSCOPY (× 12,000): Longitudinally sectioned fibers were not chosen by using the random raster scan method since this can result in all the micrographs being taken from one fiber if alignment between the fiber axis and copper grid axis occurs. An individual section was chosen randomly and then six adjacent fibers were photographed. Fibers of profile diameter less than 10 μm were rejected since they are grazing sections and contain only the peripheral 1-μm annulus (Eisenberg and Eisenberg, 1968).

In all counts from longitudinal sections the double test grid was placed at the optimal angle $\bar{\theta}$ of 19° and 71° to the muscle fiber axis; see Eq. 10. The light line spacing was 0.4 μm.

HIGH MAGNIFICATION ELECTRON MICROSCOPY (× 30,000): Micrographs were taken in the center of the same areas as the six fibers photographed at × 12,000. Areas within 1 μm of the sarcolemma were rejected. The A and I filament lengths (L_A and L_I) were measured to determine the correct volume fraction of V_A and V_I, Eq. 1. Heavy points were used to determine the actual volumes of I and A bands in each micrograph (P_I) and (P_A). The fine lattice with a spacing of 0.17 μm was used for point counting and intersection counting of the elements of the sarcoplasmic reticulum and T system in the same manner as for cross sections except that the test grid was at $\bar{\theta}$ = 19° and 71° to the fiber axis.

Myofibril diameters were determined by measuring the mean profile length from the longitudinal sections and using Eq. 16.

Z LINE WIDTH: The Z line width was measured with a measuring magnifier on longitudinally sectioned muscle at 30,000 magnification. The dense fuzzy matrix adhering to the Z line is of variable amount and obscures the filaments beneath introducing subjective estimates into the measurement. Therefore several observers measured the Z widths from the same 150 micrographs on two different days to test for reproducibility.

COMPUTATIONS: Computations were made in the interactive language APL*PLUS using an IBM 360/91 computer. The assistance of Mr. C. Clausen with programing statistical and histogram routines is gratefully acknowledged. Filing the data in disk storage allowed rapid retrieval (less than 1 s) and aided quick calculation.

RESULTS

Our primary interest was to measure the volumes, surface areas, and dimensions of the cytological components of the soleus muscle fibers in adult guinea pig in order to characterize the "average slow-twitch fiber." A large part of our work involved the application of stereological techniques, which assume that tissue is randomly oriented, to muscle tissue whose fibrils are highly oriented. We did not feel justified in assuming a priori the

degree to which any organelle or component within muscle was oriented without empirical and theoretical analysis because an incorrect assumption about orientation would introduce systematic errors into the results. We therefore analyzed orientation effects on the components in muscle by repeating the stereological analysis at two known sectioning angles, namely longitudinal ($\phi = 0°$) and cross ($\phi = 90°$). Any differences in resultant data are attributable to systematic errors caused by the orientation effect which can then be corrected.

Orientation Effects

Tables I–V present measurements of the cytological components of the muscle tissue sectioned at the two different orientations. Student's t test was applied to determine the probability level at which the data from the two orientations differed significantly. It is readily seen that there is good agreement for most of the values of volume density This is to be expected since estimates of the volume density of anisotropic components do not depend on section orientation, Eq. 7. Surprisingly, there are no significant ($P \geq 0.05$) differences between estimates of the surface density parameters made at the different sectioning angles, even though these estimates are expected to be sensitive to the sectioning angle. For fully oriented surfaces a difference of 40% would be predicted between Eqs. 13 and 14; see Fig. 2 for the curve relating the orientation angle to surface density estimates of cylinders.

Measurement of Components

In the following sections we present our measurements of the components of the soleus muscle of the guinea pig, along with a brief discussion of the reliability of the results.

The major sources of systematic errors have already been considered. The overall decrease in volume caused by fixation and embedding (−10%), section compression (−5%), aberration distortion (+2%), and printing (+1%) amounted to approximately −12% and was ignored because we do not know whether all components shrink to the same extent. Eqs. 13 and 14 allow correction to be made for systematic errors which the orientation of the surfaces would have produced. The errors due to section thickness effects have been considered negligible.

The analysis of muscle was made from five animals with 30 micrographs taken from each, yielding a total of 150 micrographs. The mean values from each of the five animals have been calculated and we present our data as the mean from the five animals with $n = 5$. All the data in this paper, whether measuring volume fraction, surface density, or length, is expressed as the mean(± 1 SEM) with $n = 5$ animals. Typical measurements from six micrographs from one block would give a relative SE of 15% (standard error/mean; $n =$ 6 micrographs) and measurements from one animal would give a relative SE of 7% ($n = 30$ micrographs from 5 blocks). For the chosen statistical presentation the typical relative SE is 7% ($n = 5$ animals).

Blood Vessels

The small blood vessels that are found between fascicles and the capillaries are dispersed between the muscle fibers (see Fig. 3). The blood vessel volume, V_B per unit volume of muscle fiber V_F, (V_B/V_F) is 2.05 ± 0.37%. Note that this volume is not expressed per unit volume of whole muscle tissue (Table I) since we have not been able to control the absolute size of the extracellular space during fixation and embedding.

Muscle Fibers

The arrangement of the muscle fibers in cross section ($75° < \phi < 90°$) is shown in Fig. 3. The A and I bands are readily identified with the light microscope. The fibers are not circular in cross-sectional profile but are irregular polyhedrons of characteristic dimension D. There was good agreement between D determined from longitudinal and cross-section material, being 33.0 ± 2.2 μm and 34.5 ± 1.1 μm, respectively, in Epon-embedded material (Table I).

A right circular cylinder of unfolded membrane with diameter D would have a surface of πDh and a volume of $\pi D^2h/4$, where h is the length. The surface-to-volume ratio would be $4/D$. We measured $D = 34 \pm 3$ μm and thus expect the surface-to-volume ratio to be 0.01 ± 0.2 $\mu m^2/\mu m^3$. The ratio of the sarcolemmal area to the muscle fiber volume S_F/V_F was measured directly as 0.12 ± 0.01 $\mu m^2/\mu m^3$. This suggests that there is little or no folding of the sarcolemma at the mean diameter and mean sarcomere length (3.4 μm), a finding which was confirmed by the appearance

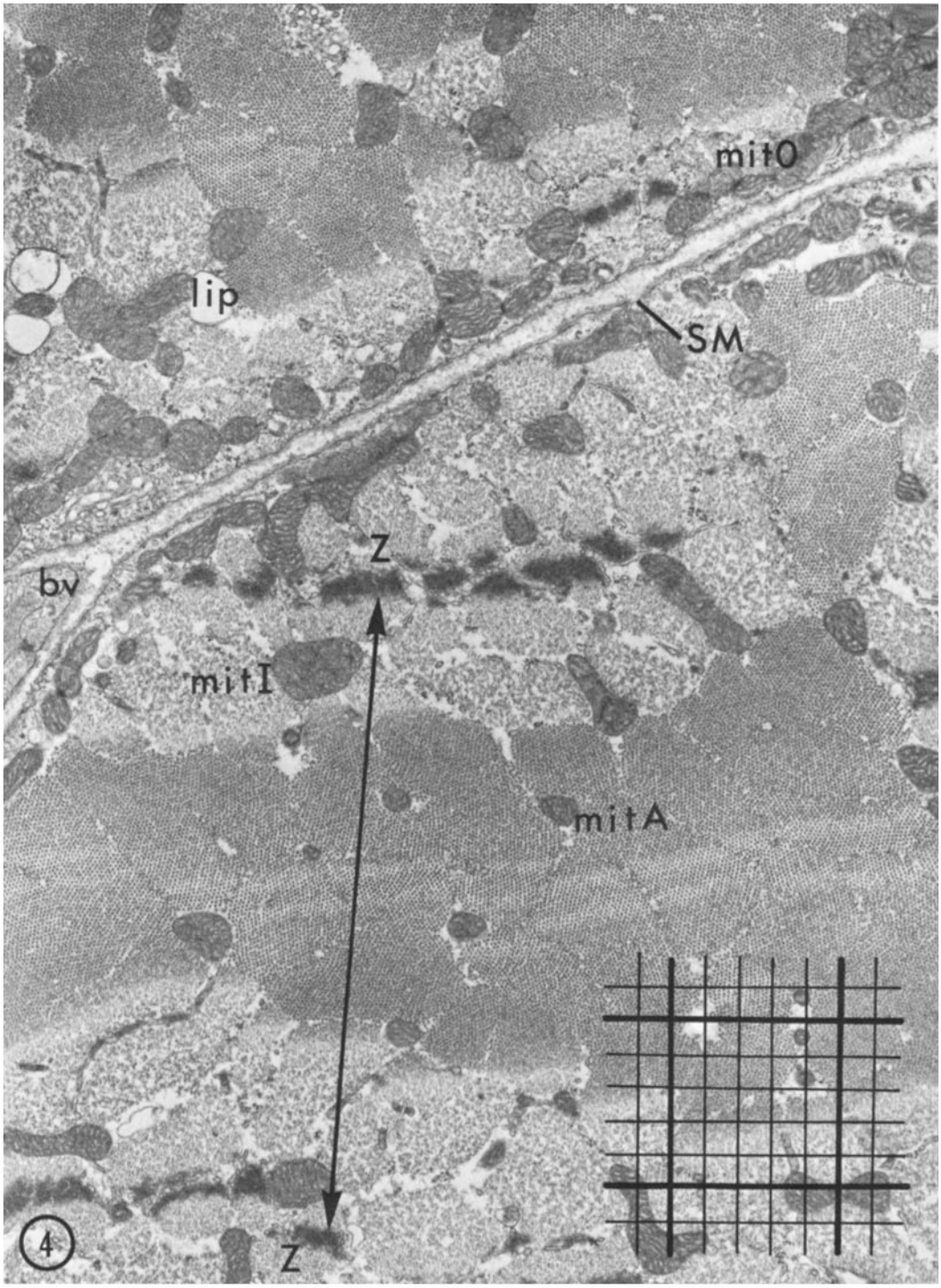

FIGURE 4 Oblique cross section of soleus muscle from the guinea pig showing parts of two fibers and a capillary (*bv*). Note the peripheral accumulation of mitochondria (*mitO*) near the sarcolemma (*SM*), the numerous, large mitochondria in the I band (*mitI*) and small mitochondria in the A band (*mitA*), and the sarcomere repeats between Z disks (*Z*). A portion of the double-test grid is shown in the lower right-hand corner. The fine lines are spaced $d = 0.4$ μm apart and the heavy lines are $5\ d = 2$ μm apart. The grid is randomly oriented to the micrograph. × 12,000.

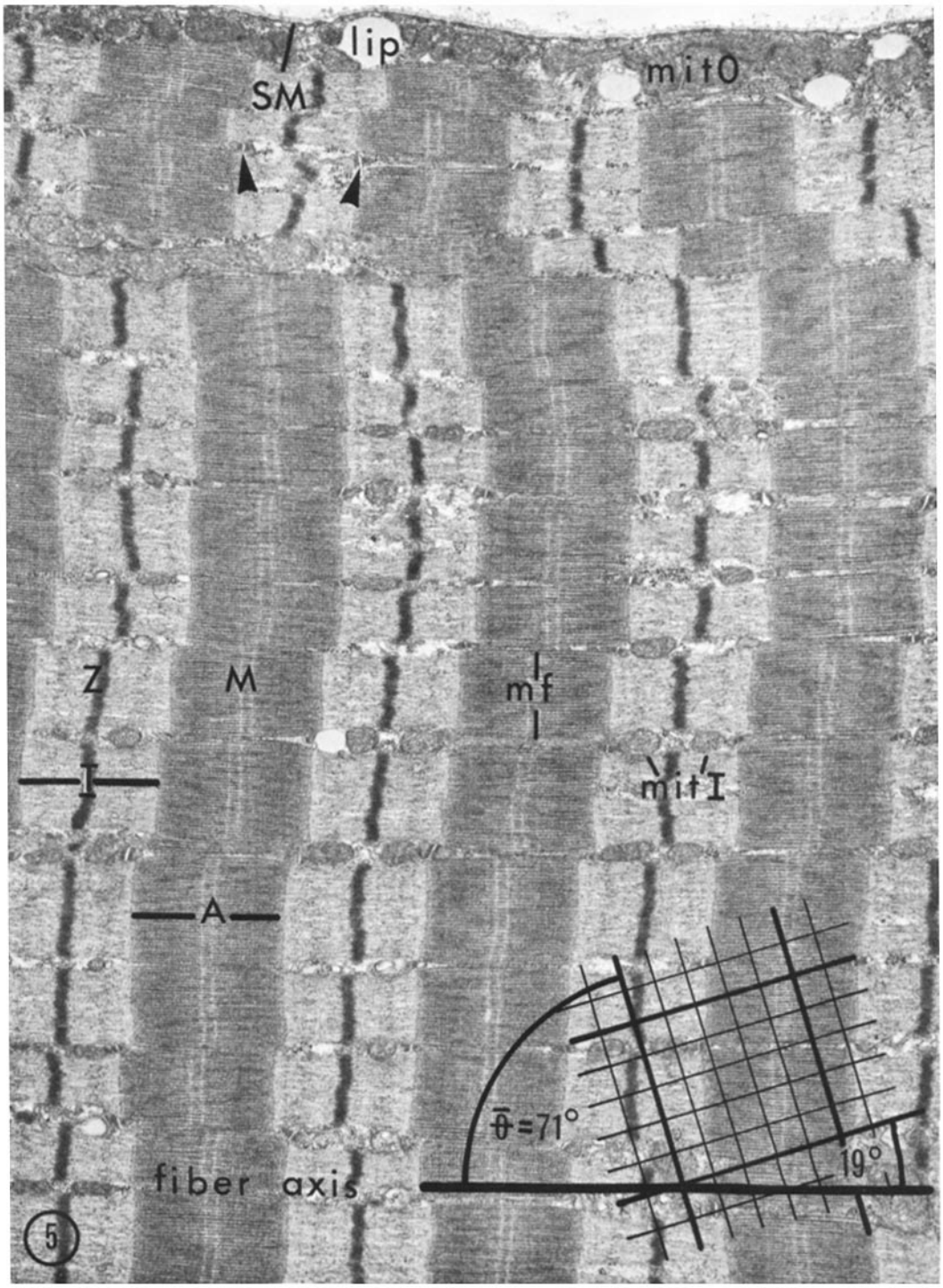

FIGURE 5 Longitudinal section through part of a soleus muscle fiber of the guinea pig. The lipid droplets (*lip*) and mitochondria (*mitO*) lie close to the sarcolemma (*SM*). The dense Z line (*Z*), moderate M line (*M*), dark A band (*A*), and light I band (*I*) give the fiber a regularly striated appearance. Arrows point to the triads located at the junction of the A and I bands, between some, but not all myofibrils (*mf*). The mitochondria in the I band (*mitI*) are often paired and A-band mitochondria are sparse. A portion of the test grid is shown oriented at the optimal angle $\bar{\theta}$ = 19° and 71° to the fiber axis. Light line spacing d = 0.4 μm. × 12,000.

TABLE I

Quantitative Data of Various Components in Guinea Pig Soleus Muscle

Component in muscle fiber (F)	Parameter	Symbol	Magnification	Longitudinally sectioned muscle* ($\phi = 0°$)	Cross-sectioned muscle* ($90° = \phi$)	Units
Blood vessels	Volume	V_B/V_F‡	1000	—	2.05 ± 0.37	$\mu m^3/100\ \mu m^3$
Fiber diameter	Width	D	750	33.0 ± 2.2	34.5 ± 1.1	μm
Sarcolemma	Surface	S_F/V_F	12,000	—	0.116 ± 0.013	$\mu m^2/\mu m^3$
Outer 1-μm annulus	Volume	V_O/V_F	12,000	3.9 ± 0.5§	10.3 ± 0.4§	$\mu m^3/100\ \mu m^3$
Sarcomere	Length	S	12,000	3.4 ± 0.2	—	μm
A Band	Volume	V_A/V_F	12,000	52.6 ± 2.9	48.8 ± 1.9	$\mu m^3/100\ \mu m^3$
I Band	Volume	V_I/V_F	12,000	47.8 ± 2.5	51.2 ± 1.9	$\mu m^3/100\ \mu m^3$
Myofibril diameter	Width		30,000	1.06 ± 0.08	1.05 ± 0.04	μm
Z Line	Width	Z	30,000	1420 ± 30	—	Å
Nucleus	Volume	V_{nuc}/V_F	1000	—	0.87 ± 0.25‖	$\mu m^3/100\ \mu m^3$
			12,000	—	0.86 ± 0.20	$\mu m^3/100\ \mu m^3$

* Results are mean ± standard error. In all cases the standard error has been calculated with $n = 5$, since five animals were used. In each animal at least 15 fibers were examined with many observations on each (see Methods).

‡ In the International Stereological symbolism the volume fractions would be denoted by V_{V_B}.

§ Significant difference ($P < 0.01$). All other paired data in this table have ($P < 0.3$).

‖ Correction for section thickness (Holmes) effect of 0.67 × has been applied.

of the tissue (see Figs. 4 and 5). Dependence of the sarcolemmal area on sarcomere length (Valdiosera et al., 1973) was not examined. We did not include the subsarcolemmal vesicles in our estimates.

The peripheral annulus of the muscle fiber contains a higher concentration of mitochondria. It was therefore necessary to measure the volume of the outer 1-μm annulus of muscle fiber. The volume of this annulus would be 11% of the volume of a 34-μm diameter fiber. The cross-sectioned material was sampled randomly and the volume of the outer annulus (V_O/V_F) was determined experimentally as 10.3 ± 0.4% in good agreement with the calculated value. However, in longitudinal sections a necessarily nonrandom method was used to choose the area of the fiber photographed to avoid the structural gradient in the periphery. The method skewed against selection of the periphery and hence the figure for V_O/V_F determined from longitudinal sections (3.9 ± 0.5%) is a biased estimate, significantly different ($P < 0.01$) from the figure expected theoretically or measured from cross sections (see Table I).

The muscles were all tied to a bar during fixation in the hope of achieving a constant sarcomere length. In fact, the mean sarcomere length was 3.4 ± 0.2 μm (mean ± standard error, with $n = 5$ animals in which 150 sarcomeres were measured). Within any one block of tissue the sarcomere length was fairly constant at 3.4 ± 0.04 μm ($n = 6$ fibers). The ratio of the volume of A band (V_A) and I band (V_I) vary with sarcomere length. However, the muscle volume (V_F) remains constant during contraction (Elliott et al., 1963) so that $V_F = V_I/V_F + V_A/V_F = 100\%$ at all sarcomere lengths.

Myofibril Diameter

The myofibril is a highly oriented bundle of filaments whose shape is most clearly seen in cross section at the level of the Z line (Fig. 6) because the sarcoplasmic reticulum, which is most abundant in that region, delineates the myofibril. The myofibrils are irregular polyhedrons assumed to be approximately circular in cross section for this analysis. The characteristic width of the myofibril was determined directly from cross-sectioned muscle ($\phi = 90°$) to be 1.05 ± 0.04 μm, whereas by the indirect method of mean profile length ($\bar{L}$) determined from longitudinally sectioned muscle ($\phi = 0°$), the myofibril width was 1.06 ± 0.08 μm (see Table I). The two methods agree closely, suggesting that the myofibrils are indeed nearly circular and that either method may be used for the determination of myofibril diameter.

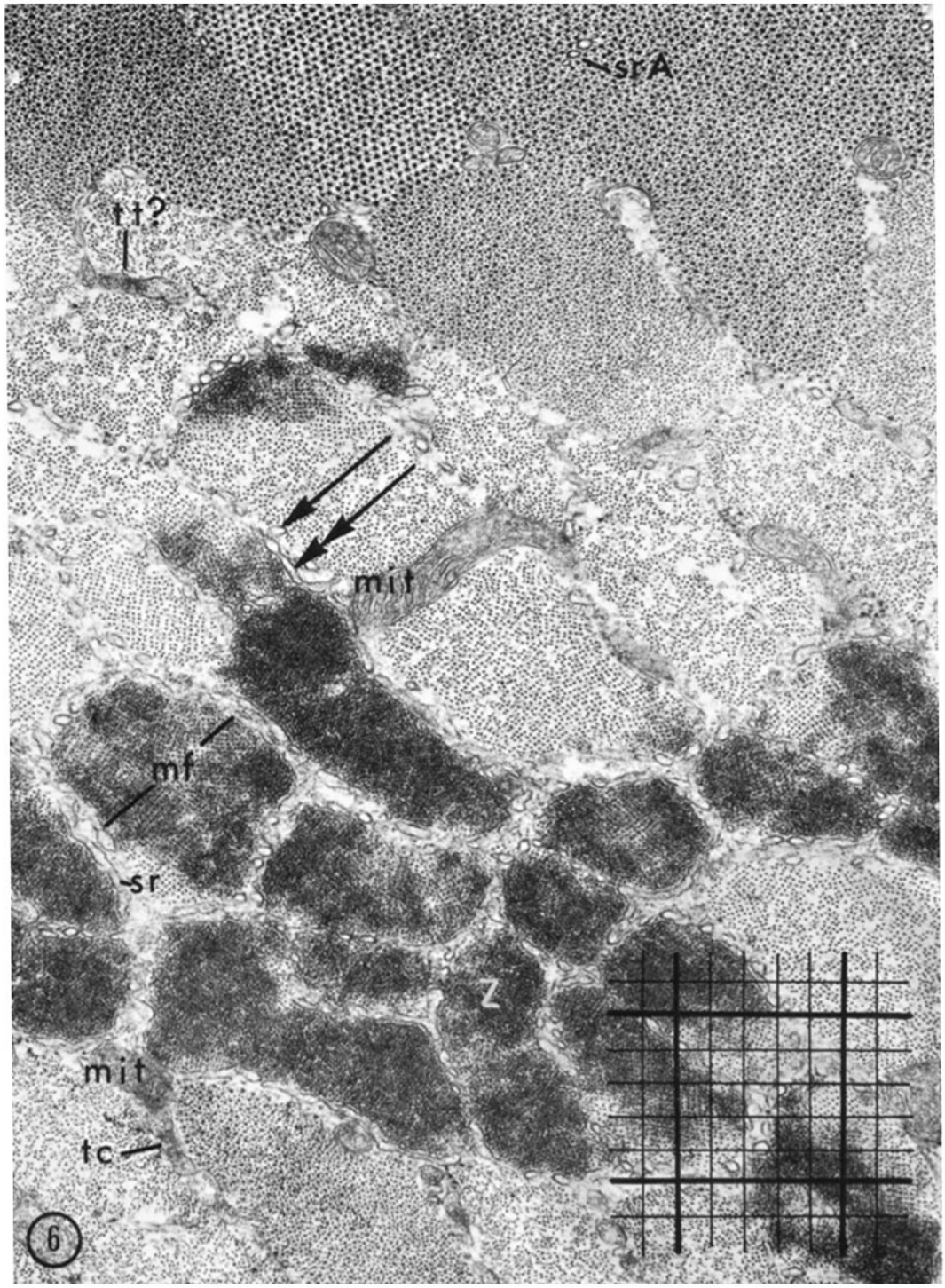

FIGURE 6 Cross section of soleus muscle showing part of one fiber. Note the dark Z disk (*Z*) broken into myofibrils (*mf*) by tubules of sarcoplasmic reticulum (*sr*) which are sectioned transversely (single arrow) and obliquely (double arrow). The mitochondria (*mit*) in the I band run transversely and can sometimes be confused with terminal cisternae (*tc*). Oblique sectioning of the tc can obscure a transverse tubule (*tt*?). The sarcoplasmic reticulum is abundant in the Z and I bands but sparse in the A band (*srA*), a portion of the test grid is shown randomly oriented to the micrograph. The fine lines are spaced $d = 0.17$ μm apart and the heavy lines are $5\,d = 0.8$ μm apart. × 30,000.

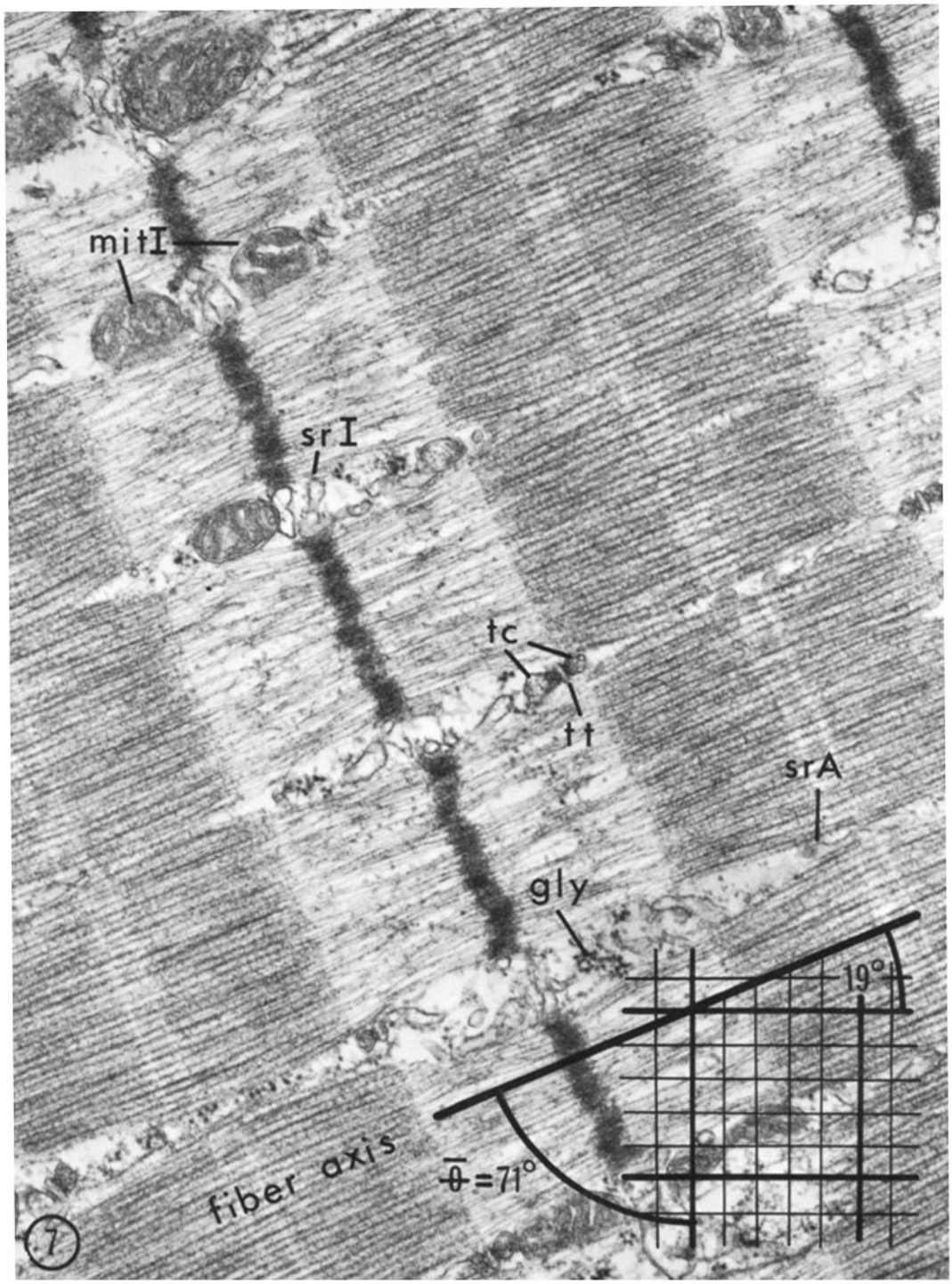

FIGURE 7 Longitudinal section through a few myofibrils of the soleus muscle of the guinea pig. Note the paired mitochondria in the I band (*mitI*). The sarcoplasmic reticulum is abundant in the I band (*srI*) and does not run parallel with the filaments. The triad consists of a central T tubule (*tt*) flanked by terminal cisternae (*tc*). The reticulum in the A band (*srA*) is sparse. Glycogen granules, *gly*. A portion of the double-test lattice is shown oriented at the optimal angle $\bar{\theta}$ = 19° and 71° to the fiber axis. The fine line spacing d = 0.17 μm. × 30,000.

Z Line Width

The term "Z line" is a misnomer, since the Z structure is in fact a thin disk and only appears as a line when longitudinally sectioned (Fig. 7). In cross section (Fig. 6) the Z disk appears as a plane fractured into myofibrils by gaps containing the sarcoplasmic reticulum. The volume of the Z disk could be determined from the muscle sectioned at any angle. However, the Z line width, measured in longitudinal sections, has often been used as an indication of fiber types and has therefore been measured. The width of the Z line in longitudinally sectioned muscle varies considerably and an attempt was made to use a measurement which would reveal this variation in an unsubjective manner (see Methods). One observer measuring the same micrographs on different days obtained means differing by 100 Å. When three observers measured the same micrographs on 2 days the mean Z line width was found to range between 1320 Å and 1490 Å, with a mean of 1420 ± 30 Å (n = 6). In the plane of the Z disk, the Z disk itself accounts for about 80% of the volume and the gaps between myofibrils fill the remaining 20%.

Muscle Nuclei

The muscle nuclei are elongated ellipsoids lying in the cell periphery. The volume fraction of the nuclei was estimated as V_{nuc}/V_F = 1.3 ± 0.4% by light microscopy and 0.86 ± 0.20% by electron microscopy. The overestimation in the light microscope measurement is caused by section thickness (Holmes, 1927). Underwood (1970, p. 174) gives an equation (6.52) which is appropriate under certain circumstances for calculating the true volume fraction V_V, given the projected areal fraction A'_A. Muscle nuclei may be taken to be cylinders of diameter (N) and the section thickness (t), then

$$V_V = A'_A\left(\frac{N}{N+t}\right). \quad (17)$$

Since the diameter of the nucleus is about 2 μm and the section thickness is 1 μm, the estimate of V_{nuc}/V_F made from the light microscope must be corrected by a factor of 0.67. The nuclear volume fraction at the light microscope level thus becomes 0.87% which then agrees with the electron microscope result (see Table I).

Lipid Droplets

Lipid droplets are sometimes found in soleus muscle fibers (Figs. 4 and 5). The lipid droplet volume fraction V_{lip}/V_F = 0.20 ± 0.06% with good agreement from cross-sectioned and longitudinally sectioned material (see Table II). The lipid droplets were preferentially distributed in the outer 1-μm annulus, V_{lipO}/V_O = 0.7 ± 0.3%. It is possible that the lipid volume has been underestimated because lipids are not well preserved with glutaraldehyde as a primary fixative, and because lipid droplets may not have been recognized in sections which just grazed the surface of the droplet.

Mitochondria

The total mitochondrial volume density in soleus muscle, V_{mit}/V_F = 4.85 ± 0.66%, a figure determined from longitudinal or cross-sectioned muscle observed at × 12,000. The mito-

TABLE II

Distribution of the Lipid Droplets within Soleus Fibers

Component	Volume symbol	Longitudinally sectioned muscle* (ϕ = 0°), μm³/100 μm³	Cross-sectioned muscle* (ϕ = 90°), μm³/100 μm³
Lipid in outer 1-μm annulus (O) of fibers	V_{lipO}/V_O	0.71 ± 0.29	0.63 ± 0.17
Lipid in core (C) of fibers	V_{lipC}/V_C	0.12 ± 0.02	0.18 ± 0.03
Total lipid in muscle (F)	V_{lip}/V_F	0.18 ± 0.04‡	0.22 ± 0.04

* All data from × 12,000 with mean ± standard error (n = 5) as in Table I. All paired data have significant difference of ($P < 0.2$).

‡ Value corrected for underestimate of V_O/V_F in Table I.

TABLE III

Distribution of Mitochondria within Soleus Fibers

Component	Volume symbol	Longitudinally sectioned muscle* (ϕ = 0°), $\mu m^3/100\ \mu m^3$	Cross-sectioned muscle* (ϕ = 90°) $\mu m^3/100\ \mu m,^3$
Mitochondria in outer 1-μm annulus (O) of fiber	V_{mitO}/V_O	18.6 ± 1.87	19.1 ± 2.5
Mitochondria in A band of core (C)	V_{mitA}/V_C	0.87 ± 0.17	0.50 ± 0.10
Mitochondria in I band of core (C)	V_{mitI}/V_C	2.76 ± 0.18	3.04 ± 0.27
Mitochondria in core (C)	$V_{mit(I+A)}/V_C$	3.63 ± 0.25‡	3.54 ± 0.29‡
Total mitochondria in muscle (F)	V_{mit}/V_F	4.87 ± 0.38§	4.83 ± 0.54

* All data from × 12,000 with mean ± standard error (n = 5) as in Table I. All paired data have significant difference of ($P < 0.1$).

‡ Standard error calculated from $\sqrt{SE_1^2 + SE_2^2}$.

§ Value corrected for underestimate of V_O/V_F in Table I.

chondria are not randomly dispersed throughout the fibers but are found mostly in two locations, the peripheral annulus and the I band (see Table III).

The peripheral annulus of the muscle fiber obviously contains a high concentration of mitochondria (Figs. 4 and 5). Chains of elongated mitochondria lie longitudinally just under the sarcolemma. Larger groups of mitochondria were noted close to nerve terminals and nuclei and near some regions of capillaries. The size of the peripheral annulus was determined by measuring the volume of mitochondria in the outer 1-μm annulus, and in another annulus ranging from 1 to 2 μm below the fiber edge. The values from the two outer annuli were compared with the remaining core at depths greater than 2 μm. The mitochondrial volume in the 1–2-μm annulus was only slightly higher than that in the core, and therefore the peripheral annulus was defined as the outer 1 μm whose symbol is V_O. The mitochondrial volume in the periphery V_{mitO}/V_O = 18.6 ± 1.9% for ϕ = 0° and 19.1 ± 2.5% when ϕ = 90°.

The mitochondrial volume in the core is given by V_{mit}/V_C = 3.6 ± 0.4% and was not significantly different in cross- and longitudinally sectioned material. The histograms (Fig. 8) show the distribution of mitochondrial volume in many fibers from both sectioning angles. The mitochondrial volume in the I band as a fraction of the volume of the core (V_{mitI}/V_C) is 2.8 ± 0.2% for ϕ = 0° and 3.0 ± 0.3% for ϕ = 90°. This is approximately four times the mitochondrial volume in the A band (V_{mitA}/V_C) which is 0.9 ± 0.2% for ϕ = 0° and 0.5 ± 0.1% for ϕ = 90°. The mitochondria

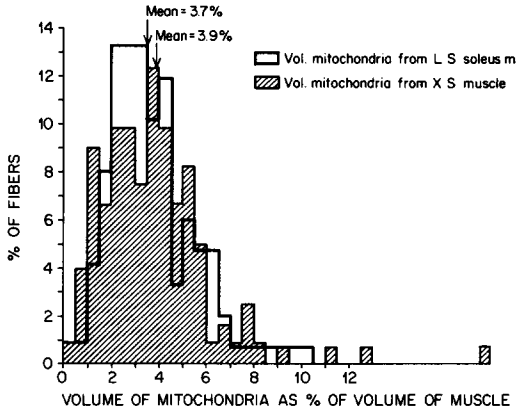

FIGURE 8 Histograms of the volume of mitochondria of soleus muscle fibers expressed as a percentage of the core, $V_{mit(I+A)}/V_C$. The mitochondrial volume in longitudinally sectioned muscle (*LS*) has a mean of 3.7% (n = 150 fibers). The cross-sectioned muscle (*XS*) has a mean of 3.9% (n = 122 fibers). Corrections for the spatial gradients within striation patterns were applied (Eq. 15) but the cross-sectioned muscle is subject to larger error (see text).

are most frequently found transversely oriented in the I band with 55.2 ± 4.3% of the profiles occurring as pairs (Fig. 5) and 27.8 ± 2.2% as singles beside the Z line. The remaining 17% of the mitochondrial profiles are longitudinally oriented alongside the fibrils in both the I and A bands.

The mitochondrial distribution might be expected to vary with sarcomere length if shortening were able to force mitochondria from the I band into the A band. The volume of the mitochondria

in the I band stayed constant down to sarcomere lengths of about 2.7 μm from a mean sarcomere length of 3.4 μm; below this length there was a decrease of mitochondria in the I band and a corresponding increase in the A band.

Sarcoplasmic Reticulum and the Transverse Tubular System

Muscle fibers contain extensive networks of small tubules which enmesh the myofibrils. The membranes of these tubules were first thought to be homologous to the endoplasmic reticulum, and the entire network was named the sarcoplasmic reticulum (Bennett and Porter, 1953). Subsequently, Andersson-Cedergren (1959) found a distinct part of the network which lay in the transverse plane called the transverse tubular system (T system). (See Peachey, 1970 for a review.)

Sarcoplasmic Reticulum in the I Band

The tubules of the sarcoplasmic reticulum in the I band are the most abundant of all the components of the sarcoplasmic reticulum. The small tubules are elliptical in profile with a minor axis of 547 ± 130 Å (mean ± standard deviation, $n = 70$) and a major axis of approximately 800 Å. The tubules form a lace-work pattern around the myofibrils in the I band (Figs. 1 and 6) as has been reported previously (Tomanek et al., 1973), and one might imagine that this meandering and branching of the tubules would be best approximated by a model of randomly oriented cylinders. We have calculated our data assuming such a random model (Table IV). We also consider the model given by Weibel, 1972, which assumed fully oriented parallel cylinders (Table V).

The volume density of the tubules of the sarcoplasmic reticulum in the I band, V_{srI}/V_F, is 1.72 ± 0.12% from longitudinal sections and 2.23 ± 0.21% from cross sections of muscle. These values are not significantly different because of the large standard error; however, the errors caused by section thickness effects would be smaller in the cross-section profile of the tubules, and therefore 2.23 ± 0.21% is probably a more reliable estimate. However, for compilation of the summary Table VI, we take the mean value from the two orientations, 1.97 ± 0.24%.

The calculation of the surface density depends on the orientation of the tubules, and so the surface density of the I band sarcoplasmic reticulum has been calculated for both the random and fully oriented cases (Table V). The random model gives the surface density of the sarcoplasmic reticulum in the I band as 0.51 ± 0.04 $\mu m^2/\mu m^3$ from longitudinal section and 0.66 ± 0.06 $\mu m^2/\mu m^3$ from cross section. These figures are significantly different ($P < 0.05$). However, calculation using the fully oriented model increases the significance of the difference ($P < 0.1$), namely 0.57 ± 0.02 $\mu m^2/\mu m^3$ from longitudinal section and 0.52 ± 0.02 $\mu m^2/\mu m^3$ from the cross section. Neither the "random" nor "fully oriented" models fit well with the data (Fig. 2) and a partially oriented model seems to be the best approximation. We have not been able to determine the theoretical

TABLE IV

Volume of the Sarcoplasmic Reticulum and T System in Soleus Fibers

Component	Volume symbol	Longitudinally sectioned muscle* ($\phi = 0°$), $\mu m^3/100\ \mu m^3$	Cross-sectioned muscle ($\phi = 90°$), $\mu m^3/100\ \mu m^3$	P
I Band sarcoplasmic reticulum	V_{srI}/V_F‡	1.72 ± 0.12	2.23 ± 0.21	<0.1
A Band sarcoplasmic reticulum	V_{srA}/V_F	0.51 ± 0.08	0.51 ± 0.08	1.0
Terminal cisternae	V_{tc}/V_F	0.92 ± 0.07	1.15 ± 0.18	<0.3
Total sarcoplasmic reticulum	$V_{(srI + srA + tc)}/V_F$	3.15 ± 0.16§	3.89 ± 0.29§	<0.05
T System	V_{tt}/V_F	0.14 ± 0.01	0.013 ± 0.003	<0.001

* All data from × 30,000 with mean ± standard error ($n = 5$) as in Table I.

‡ V_F is the volume of the muscle fiber.

§ Calculated from $\sqrt{SE^2_1 + SE^2_2 + SE^2_3}$.

TABLE V

Comparison of the Surface Density of Sarcoplasmic Reticulum and T System Calculated from Different Models

Component in muscle fiber (F)	Surface symbol	Random orientation* Longitudinally sectioned muscle (ϕ = 0°), $\mu m^2/100\ \mu m^3$	Random orientation* Cross-sectioned muscle (ϕ = 90°), $\mu m^2/100\ \mu m^3$	Partial‡ orientation, $\mu m^2/100\ \mu m^3$	Full orientation§ Longitudinally sectioned muscle (ϕ = 0°), $\mu m^2/100\ \mu m^3$	Full orientation§ Cross-sectioned muscle (ϕ = 90°), $\mu m^2/100 \mu m^3$
Sarcoplasmic reticulum in the I band	S_{srI}/V_F‖	51.3 ±3.4¶	65.7 ±6.1¶	56.4 ±7.0	56.9 ±3.7**	51.6 ±4.8‡‡
Sarcoplasmic reticulum in the A band	S_{srA}/V_F	15.5 ±2.1¶	18.5 ±2.8¶	16.4 ±3.5	17.2 ±2.3**	14.5 ±2.2‡‡
Terminal cisternae	S_{tc}/V_F	21.9 ±1.5¶	25.9 ±4.6¶	23.4 ±4.6	17.2 ±1.2‡‡	28.7 ±4.1**
T System	S_{tt}/V_F	6.4 ±0.5¶	0.22 ±0.04¶	?	5.0 ±0.4‡‡	0.024 ±0.004**

* Random orientation means that all angles between the tubules axes and the fiber axis are equally probable.

‡ Partial orientation of the tubules is a situation between random and full orientation.

§ Full orientation means that the angles between all the tubule axes and the fiber axis are the same, i.e., the tubules are parallel to each other.

‖ In the International Stereological symbolism surface densities would be denoted by $S_{V_{srI}}$.

¶ See text Eq. 7.

** See text Eq. 14.

‡‡ See text Eq. 13.

correction factor needed in the partially oriented case and so arbitrarily choose the mean of the four calculated values in Table V as the best estimate, namely 0.56 ± 0.07 $\mu m^2/\mu m^3$.

The surface-to-volume ratio S_{srI}/V_{srI} for the sarcoplasmic reticulum in the I band is about 23 $\mu m^2/\mu m^3$. A cylinder with this surface-to-volume ratio would have a diameter of approximately 1500 Å, which is twice as big as the actual measured diameter. The discrepancy could be explained by assuming that the sarcoplasmic reticulum tubules are meandering cylinders or by assuming some more complex geometry such as a fenestrated cisterna.

Sarcoplasmic Reticulum in the A Band

The best estimate for the volume density of the sarcoplasmic reticulum in the A band is 0.51 ± 0.08% and for the surface density obtained from the partially oriented model is 0.16 ± 0.04 $\mu m^2/\mu m^3$ (Table V). Hence the surface-to-volume ratio of the A band reticulum is 31 $\mu m^2/\mu m^3$, which correlates to a simple cylinder of diameter approximately 1200 Å, which is about twice the actual measured value, again implying a more complex geometry exists.

Terminal Cisternae

The terminal cisternae are recognized by their location adjacent to the T system in the zone where the A and I filaments overlap and also by the granular content in the lumen of the cisternae (Fig. 7). In muscle cut at cross section, a grazing slice through the cisternae can be confused with a mitochondrial profile (Fig. 6). This confusion would cause overestimation of the volume density of the cisternae, and indeed the figure from cross sections is slightly higher, 1.15 ± 0.18%, than the figure of 0.92 ± 0.07% from longitudinal sections ($P < 0.3$; see Table IV).

The surface membranes of the cisternae are randomly oriented as judged by the lack of dependence on the test grid angle θ and also by the good agreement in the data from longitudinal section and cross section calculated from the isotropic model: 0.22 ± 0.04 and 0.26 ± 0.05 $\mu m^2/\mu m^3$, respectively. Table V shows that calculation for a fully oriented model with the axis perpendicular to the fiber axis does not fit at all. In fact, the orientation "correction" factor increases the disparity between longitudinal and cross-sectional estimates.

The surface-to-volume ratio of the terminal

cisternae is given by 23.8 $\mu m^2/\mu m^3$ from longitudinal section and 22.5 $\mu m^2/\mu m^3$ from cross section. The equivalent diameter for the cylinder with this ratio is approximately 1700 Å compared with the 1300 Å actually measured. The difference in figures is probably the result of bending which occurs as the cisternae surround the myofibrils.

Transverse Tubular System

The transverse tubules are readily recognized in longitudinally sectioned muscle (Figs. 5 and 7) but are almost totally obscured by the opaque terminal cisternae when the muscle is sectioned transversely (Figs. 4 and 6). This identification problem is apparent in the data which shows a 10-fold discrepancy between the cross-sectional and longitudinal results (Table IV). We are therefore forced to rely on the data obtained from longitudinal sections alone. The volume density is 0.14 ± 0.01% and the surface density is 0.064 ± 0.005 $\mu m^2/\mu m^3$. The T system tubules have been considered isotropic since there was no significant dependence of intersection counts on the test grid angle θ. The ratio of the surface to volume of an ellipse is given approximately by

$$\frac{S}{V} = \frac{2}{ab}\sqrt{\frac{a^2 + b^2}{2}}, \qquad (18)$$

where a and b are the major and minor axes, and are approximately 200 Å and 500 Å, respectively for the T tubules. These values for a and b give S/V = 76 $\mu m^2/\mu m^3$, which is higher than the measured value of 46 $\mu m^2/\mu m^3$ and again may indicate that the tubules are bent.

DISCUSSION

Stereological Techniques

The point counting techniques of stereology proved to be fast, reliable, and accurate when applied to muscle tissue analysis. The fibers and myofibrils are highly oriented with a pronounced longitudinal axis. The results from both cross and longitudinal sections to this axis were identical for the volume and surface densities of most cellular components. The major exceptions are the T system which can only be recognized in longitudinal sections, and the Z line width which can only be determined from longitudinal sections. It seems satisfactory then to use only longitudinal sections in the future analysis of cellular components in other muscles.

Our data show that the tubules of the sarcoplasmic reticulum deviate from a parallel course, but not to the extent of becoming randomly oriented. We call this situation partial orientation. We do not know how these partially oriented tubules are distributed about the axis of the fiber, and the correct theoretical analysis will depend on the particular distribution. The experimental curve (Fig. 2) for the tubules of the sarcoplasmic reticulum lies about halfway between the random and fully oriented curves, and therefore we assume that the correction for the orientation effect should also lie between the two extremes. In Table V the value given for the partial orientation is the mean value of the random and fully oriented data at both sectioning angles ($\phi = 0°$ and $\phi = 90°$). More theoretical work is needed to justify this procedure.

Measurement of Components

Z LINE WIDTH: The width of the Z line has been used to differentiate various types of skeletal muscle fibers (Gauthier, 1970). We found that that measured width varies with the subjective judgement of the observer and reproducibility is only ± 50 Å. Further, the Z width is dependent on orientation, fixation, and contraction (Landon, 1970; Kelly and Cahill, 1972). Absolute widths are not quoted by Rowe (1973) who related all lengths to a 40 nm periodicity in the I band which is equivalent to a 1400-Å width of the Z line in the slow red fiber. Tomanek et al. (1973) record the Z line width of the soleus in the guinea pig as 1205 ± 58 Å (mean ± standard deviation, n not given). Perhaps the volume of the Z band would be a more reproducible parameter to measure in the future.

VOLUME DENSITY OF COMPONENTS: The The volumetric components of the soleus muscle fiber are summarized in Table VI. The contractile proteins and sarcoplasm occupy 90% of the cell volume. The other functional activities of the cell take place in the remaining 10% of the cell volume. The nuclei (0.9%) and lipid (0.2%) are relatively rare and are preferentially distributed in the cell periphery (Tables I and II). The mitochondria are also more concentrated in the outer 1-μm annulus of the fiber (Table III). The total mitochondrial volume is 4.85% in the adult guinea pig which can be compared with the rat

TABLE VI

*Summary of Quantitative Data for Components of Soleus Muscle Fibers in the Adult Guinea Pig**

Component	Volume, $\mu m^3/100\ \mu m^3$	Surface area, $\mu m^2/100\ \mu m^3$
Lipid droplet	0.20 ± 0.06	—
Mitochondria	4.85 ± 0.66	—
Terminal cisternae	1.04 ± 0.19	23.9 ± 4.8‡
Tubules of sarcoplasmic reticulum	2.48 ± 0.26	72.8 ± 7.8§
Terminal cisternae and tubules of sarcoplasmic reticulum	3.52 ± 0.33	96.7 ± 9.2
T System	0.14 ± 0.01‖	6.4 ± 0.5‖
Sarcolemma	—	11.6 ± 1.3¶

* Data expressed as fractions of 100 μm^3 of muscle fiber; (mean ± standard error). Data pooled from five guinea pigs; 30 fibers for each animal for longitudinal sections and 15 fibers for each animal in cross sections.

‡ Calculated from random orientation model.

§ Calculated for partially oriented model.

‖ Longitudinal section data only because T system is not identifiable in cross sections of muscle.

¶ Cross section data only (see text).

which has 7.4% from cross sections and 5.7% from longitudinal sections (Stonnington and Engel, 1973). The total volume of the sarcoplasmic reticulum in the adult guinea pig was 3.5% and in the mouse soleus muscle was 2.9% (Luff and Atwood, 1971). It is worth noting that the mitochondrial and sarcoplasmic reticulum volumes are of comparable size (4.8% and 3.5%, respectively). More comparisons between the volumes of various components and functional roles will be made by us in subsequent papers in which different fiber types will be examined.

SURFACE DENSITY OF MEMBRANE COMPONENTS: The surface densities of the membrane components measured here provide some interesting data (Table VI) which has not previously been obtained in mammalian skeletal muscle. The surface area of the sarcolemma is only about twice as great as the T system surface area. This would lead one to expect that a lower membrane capacitance should be found in mammalian slow-twitch muscle than in frog fast-twitch muscle where the T system is seven times the sarcolemmal area for a 100-μm fiber (Peachey, 1965) and the capacitance is 6 $\mu F/cm^2$ for a 100-μm fiber diameter (Hodgkin and Nakajima, 1972). In fact one would predict that the capacitance of the average guinea pig soleus fiber (diameter, 34 μm) should be on the order of 3 $\mu F/cm^2$ if the specific capacitance of the T system and sarcolemma are the same, namely 2 $\mu F/cm^2$ each. This would be in line with the capacitance measured in other mammalian slow-twitch muscles (Luff and Atwood, 1972).

The total surface area of the total sarcoplasmic reticulum is 0.97 ± 0.9 $\mu m^2/\mu m^3$ in the guinea pig. In the rat, Stonnington and Engel (1973) found the surface area of the sarcotubular system in red fibers to be 1.21 ± 0.13 $\mu m^2/\mu m^3$ from longitudinal sections and twice that value from cross sections. They do not explain this discrepancy.

The surface area of the sarcoplasmic reticulum in the guinea pig is about 15 times as great as the T system (0.06 $\mu m^2/\mu m^3$) or about five times the T system and sarcolemma together (0.18 $\mu m^2/\mu m^3$).

We made some correlation between the location of components within the sarcomere and the length of the sarcomere. At short sarcomere lengths (below 2.7 μm) the mitochondria appear to be forced into the A band from their usual position in the I band. However, the amount of reticulum in either band remains constant with sarcomere length. The tubules may become more bent in the I band at shorter sarcomere lengths and hence more randomly oriented with respect to the fiber axis. In the soleus muscle both the mitochondria and the sarcoplasmic reticulum are about fourfold more extensive in the I band than in the A band.

The stereological analysis of muscle has been shown to be a powerful, cheap, and convenient method by which to obtain quantitative data from muscle fibers. Problems of orientation and structural gradients within a fiber can be overcome and accurate data obtained. The present paper describes the cytological characteristics of the average slow-twitch-oxidative fiber found in the soleus muscle of the adult guinea pig. Stereological analysis of other fiber types will allow further comparison of fiber-by-fiber histograms and this should facilitate functional correlations to be made.

We are indebted to Dr. R. S. Eisenberg for his valuable advice in the design and analysis of these experiments and for his critical review of this manuscript. Theoretical discussions with Dr. J. D. Cole were most helpful. The use of the electron micros-

copy facilities of Dr. R. F. Dunn are gratefully acknowledged.

This work was supported by a grant-in-aide from the Muscular Dystrophy Associations of America, Inc., and U. S. Public Health Service Grant GM 15759.

Received for publication 10 August 1973, and in revised form 14 November 1973.

REFERENCES

ANDERSSON-CEDERGREN, E. 1959. Ultrastructure of motor end-plate and sarcoplasmic components of mouse skeletal muscle fibre as revealed by three dimensional reconstruction from serial sections. *J. Ultrastruct. Res. Suppl.* **1**:5.

BARNARD, R. J., V. R. EDGERTON, T. FURUKAWA, and J. B. PETER. 1971. Histochemical, biochemical and contractile properties of red, white and intermediate fibers. *Am. J. Physiol.* **220**:410.

BENNETT, H. S., and K. R. PORTER. 1953. An electron microscopic study of sectioned breast muscle of domestic fowl. *Am. J. Anat.* **93**:61.

BURKE, R. E., D. N. LEVINE, F. E. ZAJAC, P. TSAIRIS, and W. K. ENGEL. 1971. Mammalian motor units: physiological-histochemical correlation in three types in cat gastrocnemius. *Science (Wash. D. C.).* **174**:709.

CLOSE, R. 1972. Dynamic properties of mammalian skeletal muscle. *Physiol. Rev.* **52**:129.

COURANT, R. 1937. Differential and Integral Calculus. Interscience Publishers Inc., New York.

DEHOFF, R. T., and F. N. RHINES. 1968. Quantitative Microscopy. McGraw-Hill Book Company, New York.

DENNY-BROWN, D. E. 1929. The histological features of striped muscle in relation to its functional activity. *Proc. R. Soc. Lond. B Biol. Sci.* **104**:371.

DUNN, R. F., and G. W. B. PREISS. 1973. Digital display of lens current for accurate calibration of the electron microscope. *In* Proceedings of the 31st Electron Microscope Society of America Meeting. C. J. Arceneaux, editor. Claitor's Publishing Co., Baton Rouge, La. 98.

EDGERTON, V. R., and D. R. SIMPSON. 1969. The intermediate muscle fiber of rats and guinea pigs. *J. Histochem. Cytochem.* **17**:828.

EISENBERG, B., and R. S. EISENBERG. 1968. Selective disruption of the sarcotubular system in frog sartorius muscle. A quantitative study with exogenous peroxidase as a marker. *J. Cell Biol.* **39**:451.

EISENBERG, B. R., A. KUDA, and J. B. PETER. 1972. Morphometric analysis of the slow-twitch fibers of the guinea pig. *In* Proceedings of the 30th Electron Microscope Society of America Meeting. C. J. Arceneaux, editor. Claitor's Publishing Co., Baton Rouge, La. 36.

ELIAS, H. 1967. Stereology—Second International Congress for Stereology. Springer-Verlag New York Inc., New York.

ELIAS, H., and A. HENNIG. 1967. Stereology of human renal glomerulus. *In* Quantitative Methods of Morphology. E. R. Weibel and H. Elias, editors. Springer-Verlag New York Inc., New York.

ELIAS, H., A. HENNIG, and D. E. SCHWARTZ. 1971. Stereology: applications to biomedical research. *Physiol. Rev.* **51**:158.

ELLIOTT, G. F., F. J. LOWY, and C. R. WORTHINGTON. 1963. An X-ray and light-defraction study of the filament lattice of striated muscle in the living state and in rigor. *J. Mol. Biol.* **6**:295.

ENGEL, W. K. 1970. Selective and nonselective susceptibility of muscle fiber types. *Arch. Neurol.* **22**:97.

GALAVAZI, G., and J. A. SZIRMAI. 1971. Cytomorphometry of skeletal muscle. *Z. Zellforsch. Mikrosk. Anat.* **121**:507.

GAUTHIER, G. F. 1970. The ultrastructure of the three fiber types in mammalian skeletal muscle. *In* The Physiology and Biochemistry of Muscle as a Food. E. J. Brisky, R. G. Cassens, and B. B. Marsh, editors. University of Wisconsin Press, Madison. **2**:103.

GAUTHIER, G. F., and H. A. PADYKULA. 1966. Cytological studies of fiber types in skeletal muscle. *J. Cell Biol.* **28**:333.

HAYASHIDA, Y., and H. SCHMALBRUCH. 1972. The size of fat particles in skeletal muscle fibers rich in mitochondria and its relation to nourishment in the rat. *Z. Zellforsch. Mikrosk. Anat.* **127**:374.

HERBENER, G. H., R. H. SWIGART, and C. A. LANG. 1973. Morphometric comparison of the mitochondrial populations of normal and hypertrophic hearts. *Lab. Invest.* **28**:96.

HILLIARD, J. E. 1967. Determination of structural anisotropy. *In* Stereology. H. Elias, editor, Springer-Verlag New York Inc., New York. 219.

HODGKIN, A. L., and S. NAKAJIMA. 1972. The effect of diameter on the electrical constants of frog skeletal muscle fibres. *J. Physiol. (Lond.).* **221**:105.

HOLMES, A. H. 1927. Petrographic Methods and Calculations. Thomas Murby and Company, London.

KELLY, D. E., and M. A. CAHILL. 1972. Filamentous and matrix components of skeletal muscle Z-disks. *Anat. Rec.* **172**:623.

KILARSKI, W. 1973. Cytomorphometry of sarcoplasmic reticulum in extrinsic eye muscles of the teleost. *Z. Zellforsch. Mikrosk. Anat.* **136**:535.

LANDON, D. N. 1970. The influence of fixation upon the fine structure of the Z-disk of rat striated muscle. *J. Cell Sci.* **6**:257.

LOUD, A. V. 1967. Quantitative estimation of the loss of membrane images resulting from oblique

sectioning. *In* Proceedings of the 25th Electron Microscope Society of America Meeting. C. J. Arceneaux, editor. Claitor's Publishing Co., Baton Rouge, La. 144.

LUFF, A. R., and H. L. ATWOOD. 1971. Changes in the sarcoplasmic reticulum and transverse tubular system of fast and slow skeletal muscles of the mouse during postnatal development. *J. Cell Biol.* **51**:369.

LUFF, A. R., and H. L. ATWOOD. 1972. Membrane properties and contraction of single muscle fibers in the mouse. *Am. J. Physiol.* **222**:1435.

MOBLEY, B. A., and E. PAGE. 1972. The surface area of sheep cardiac purkinje fibres. *J. Physiol. (Lond.).* **220**:547.

OGATA, T., and F. MURATA. 1969. Cytological features of three fiber types in human striated muscle. *Tohoku J. Exp. Med.* **99**:225.

PAGE, S. G., and H. E. HUXLEY. 1963. Filament lengths in striated muscle. *J. Cell Biol.* **19**:369.

PELLEGRINO, C., and C. FRANZINI. 1963. An electron microscopic study of denervation atrophy in red and white skeletal muscle fibers. *J. Cell Biol.* **17**:327.

PEACHEY, L. D. 1958. Thin sections. I. A study of section thickness and physical distortion produced during microtomy. *J. Biophys. Biochem. Cytol.* **4**:233.

PEACHEY, L. D. 1965. The sarcoplasmic reticulum and transverse tubules of the frog sartorius. *J. Cell Biol.* **25**(3, Pt. 2):209.

PEACHEY, L. D. 1968. Muscle. *Annu. Rev. Physiol.* **30**:401.

PEACHEY, L. D. 1970. Form of the sarcoplasmic reticulum and T system of striated muscle. *In* The Physiology and Biochemistry of Muscle as a Food. E. J. Brisky, R. G. Cassens, and B. B. Marsh, editors. University of Wisconsin Press, Madison. **2**:273.

PETER, J. B., R. J. BARNARD, V. R. EDGERTON, C. A. GILLESPIE, and K. E. STEMPEL. 1972. Metabolic profiles of three fiber types of skeletal muscle in guinea pigs and rabbits. *Biochemistry.* **11**:2627.

RANVIER, L. 1874. De quelques faits relatifs à l'histologie et à la physiologie des muscles striés. *Arch. Physiol. Norm. Pathol. Ser. 2.* **1**:5.

ROWE, R. W. D. 1973. The ultrastructure of Z disks from white, intermediate and red fibers of mammalian striated muscles. *J. Cell Biol.* **57**:261.

SANTA, T., A. G. ENGEL, and E. H. LAMBERT. 1972. Histometric study of neuromuscular junction ultrastructure. *Neurology.* **22**:71.

SCHIAFFINO, S., V. HANZLIKOVA, and S. PIEROBON. 1970. Relations between structure and function in rat skeletal muscle fibers. *J. Cell Biol.* **47**:107.

SHAFIQ, S. A., M. A. GORYCKI, and A. T. MILHORAT. 1969. An electron microscopic study of fibre types in normal and dystrophic muscles of the mouse. *J. Anat.* **104**:281.

SITTE, H. 1967. Morphometrische Untersuchungen an Zellen. *In* Quantitative Methods in Morphology. E. R. Weibel and H. Elias, editors. Springer-Verlag New York Inc., New York. 167.

SMITH, C. S., and L. GUTTMAN. 1953. Measurement of internal boundaries in three-dimensional structures by random sectioning. *J. Metals.* **5**:81.

STONNINGTON, H. H., and A. G. Engel. 1973. Normal and denervated muscle. *Neurology.* **23**:714.

TOMANEK, R. J., C. R. ASMUNDSON, R. R. COOPER, and R. J. BARNARD. 1973. Fine structure of fast-twitch and slow-twitch guinea pig muscle fibers. *J. Morphol.* **139**:47.

UNDERWOOD, E. E. 1968. Surface area and length in volume. *In* Quantitative Microscopy. R. T. DeHoff and F. N. Rhines, editors. McGraw-Hill Book Company, New York. 78.

UNDERWOOD, E. E. 1970. Quantitative Stereology. Addison-Wesley Publishing Co., Inc., Reading, Mass.

VALDIOSERA, R., C. CLAUSEN, and R. S. EISENBERG. 1973. Impedance of frog skeletal muscle fibers. *Biophys. Soc. Annu. Meet. Abstr.* **13**:195 *a*.

VENABLE, J. H., and R. COGGESHALL. 1965. A simplified lead citrate stain for use in electron microscopy. *J. Cell Biol.* **25** (2, Pt. 1):407.

WEIBEL, E. R. 1963. Morphometry of the Human Lung. Academic Press Inc., New York.

WEIBEL, E. R. 1969. Stereological principles for morphometry in electron microscopic cytology. *Int. Rev. Cytol.* **26**:235.

WEIBEL, E. R. 1972. A stereological method for extimating volume and surface of sarcoplasmic reticulum. *J. Microsc. (Oxf.).* **95**:229.

WEIBEL, E. R. 1973. *In* Principles and Techniques of Electron Microscopy. M. A. Hayat, editor. Van Nostrand Reinhold Company, New York. **3**:237.

WEIBEL, E. R., and H. ELIAS. 1967. Quantitative Methods in Morphology (First International Stereology Conference). Springer-Verlag New York Inc., New York.

WEIBEL, E. R., G. S. KISTLER, and W. F. SCHERLE. 1966. Practical stereological methods for morphometric cytology. *J. Cell Biol.* **30**:23.